Journal of Asian Earth Sciences 72 (2013) 164–177

Contents lists available at SciVerse ScienceDirect

Journal of Asian Earth Sciences

journal homepage: www.elsevier.com/locate/jseaes

Paleomagnetism of the late Cryogenian Nantuo Formation and paleogeographic implications for the South China Block

Shihong Zhang [a,*], David A.D. Evans [b], Haiyan Li [a], Huaichun Wu [a], Ganqing Jiang [c], Jin Dong [a], Qingle Zhao [a], Timothy D. Raub [b,1], Tianshui Yang [a]

[a] State Key Laboratory of Biogeology and Environmental Geology, China University of Geosciences, Beijing 100083, China
[b] Department of Geology and Geophysics, Yale University, New Haven, CT 06520-8109, USA
[c] Department of Geosciences, University of Nevada, Las Vegas, NV 89154-4010, USA

ARTICLE INFO

Article history:
Available online 22 November 2012

Keywords:
Paleomagnetism
Nantuo Formation
South China Block
Neoproterozoic
Global reconstruction

ABSTRACT

A new paleomagnetic pole position is obtained from the well-dated (636.3 ± 4.9 Ma) Nantuo Formation in the Guzhang section, western Hunan Province, and the correlative Long'e section in eastern Guizhou Province, South China. Remagnetization of the recent geomagnetic field was identified and removed for both sections. The hard dual-polarity, interpreted as primary, component of the Nantuo Formation, directs east–westward with medium inclinations, yielding an average pole of 9.3°N, 165°E, A_{95} = 4.3° that, for the first time, passed a strata-bound reversals test. The new data are consistent with previously published paleomagnetic data of the Nantuo Formation from Malong county, central Yunnan Province, which passed a positive syn-sedimentary fold test. Together, these sites represent shallow- to deep-water sections across a shelf-to-basin transect centered at ~33° paleolatitude. The sedimentary basin may have faced an expansive ocean toward the paleo-East. In the ~750 Ma and ~635 Ma global reconstructions, the South China Block (SCB) was best fitted in the northern hemisphere close to northwestern Australia. However, a direct SCB-northwestern Australia connection, inferred to have existed during the Early Cambrian–Early Devonian, had not formed by the time of ~635 Ma.

1. Introduction

The Nantuo Formation (~654–635 Ma) is commonly correlated as Marinoan-age glaciogenic strata in South China (Fig. 1, Jiang et al., 1996; Dobrzinski and Bahlburg, 2007; Zhang et al., 2008a). Paleomagnetic results directly from the Nantuo Formation are crucial for understanding the paleogeographic position of the South China Block (SCB) among the fragmented landmasses begat by Rodinia, and for assessing the extreme late Neoproterozoic paleoclimate changes. However, because of pervasive Mesozoic–Cenozoic remagnetization across the SCB, only a few acceptable paleomagnetic results have been obtained from the Nantuo Formation thus far (e.g., Zhang and Piper, 1997). These few results would benefit from more concrete field tests (e.g., strata-bound reversals) and from comparison with geochronologically constrained sections within tectonically unrotated domains.

Permitted by the lack of reliable paleomagnetic data directly from the Nantuo Formation, some researchers have proposed that the Nantuo glaciation might have occurred close to the equator, on the basis of a shallow remanent magnetization in the Doushantuo Formation (635–551 Ma), which directly overlies the Nantuo Formation (Macouin et al., 2004), or based on moderately-inclined remanent magnetization in the Liantuo Formation (~750 Ma), which underlies the Nantuo Formation (Evans et al., 2000). However, the Liantuo Formation is ~100 million years older than the Nantuo Formation, and the Doushantuo Formation spans ~80 million years of time. Both units were deposited during time intervals that were paleomagnetically characterized elsewhere by rapid plate motion and/or geodynamic exceptionalism (Raub et al., 2007). Thus, paleomagnetic results from the Liantuo and Doushantuo formations may not provide paleolatitude constraints for the Nantuo glaciation.

In this paper, we report new paleomagnetic results directly from the Nantuo Formation in two sections that are paleogeographically separated and lithologically distinctive. On the basis of these new data and an update of the high-quality global paleomagnetic dataset, we discuss the paleogeographic position of the SCB in late Neoproterozoic global reconstructions.

2. Geological background of sampling areas

The traditionally termed 'South China Block' comprises two tectonic units, the Yangtze block (YB) in its modern northwest and the

* Corresponding author. Tel.: +86 10 82322257; fax: +86 10 82321983.
E-mail address: shzhang@cugb.edu.cn (S. Zhang).
[1] Present address: Department of Earth Sciences, University of St. Andrews, St. Andrews, SC KY16 9AL, UK.

1367-9120/$ - see front matter
http://dx.doi.org/10.1016/j.jseaes.2012.11.022

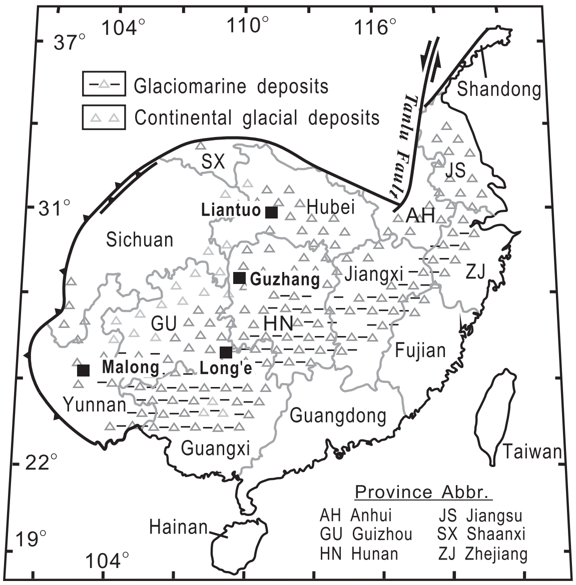

Fig. 1. Tectonic boundaries of the SCB and distribution of the Nantuo Formation. Closed squares show the paleomagnetic study locations for the Liantuo and Nantuo Formations in South China.

Cathaysia block (CB) in its modern southeast. The two continental blocks likely assembled as one tectonic entity after ~900 Ma during the Sibao orogeny (Ye et al., 2007; Li et al., 2008a). The development of the Nanhua rift basin initiated approximately along the suture zone at ~830 Ma, soon after the amalgamation (Jiang et al., 2003; Wang and Li, 2003; Li et al., 2010a,b). However, some studies suggested that the Neoproterozoic basin may represent a back-arc basin (Zhou et al., 2002; Zhao et al., 2011; Zhang et al., in press).

Unmetamorphosed Neoproterozoic strata in South China are mainly preserved on the southeastern margin of the Yangtze block and are conventionally divided into three parts (Jiang et al., 2003, 2011; Fig. 2): (1) pre-glacial volcanic and siliciclastic rocks of the Banxi Group and its equivalents, with ages ranging from ~820 Ma to 725 Ma (Wang et al., 2003; Zhang et al., 2008b,c); (2) two Cryogenian glacial diamictite intervals represented by the Chang'an/Dongshanfeng Formations and Nantuo Formation, respectively, separated by interglacial Datangpo/Xiangmeng Formations dated between ~663 and ~654 Ma (Zhou et al., 2004; Zhang et al., 2008a); and (3) postglacial marine carbonates and shales of Ediacaran strata, of which the Doushantuo Formation has been well dated as ~635–551 Ma (Condon et al., 2005; Zhang et al., 2005). The younger of the two Cryogenian glaciogenic units, the Nantuo Formation, is ~60–130 m thick in the shelf and >2000 m thick in the basin. It consists of massive and stratified diamictites and conglomerates with sandstone and siltstone beds (Jiang et al., 1996). Diamictites contain abundant bullet-shaped and striated clasts, dropstones and lonestones (HNBGMR, 1988; Jiang et al., 1996; Dobrzinski and Bahlburg, 2007; Zhang et al., 2011). A 5-m-thick cap carbonate, commonly referred to as Member I of the Doushantuo Formation, directly overlies the glacial diamictites of the Nantuo Formation and serves as a distinctive marker bed across the Nanhua basin (Jiang et al., 2006a,b).

Our new paleomagnetic investigations were carried out at two sections. One section is located near Guzhang (Fig. 2A and C, near 28°30.1′N, 109°50.3′E), along the highway from Zhangjiajie to Jishou, western Hunan Province. The Nantuo Formation in this section is about 130 m thick, including ~20 m of laminated red silty sandstone and mudstone in its lower part (Fig. 2C). A tuff bed just below the boundary between the Nantuo Formation and underlying interglacial deposits of the Xiangmeng Formation is dated at ~654 ± 3.8 Ma and a fallout tuff bed ~8 m higher, within diamictite beds of the basal Nantuo Formation, is dated at 636.3 ± 4.9 Ma, both by U–Pb SHRIMP on zircon (Zhang et al., 2008a). Our paleomagnetic sampling sites, ~12 m higher than the younger dated tuff bed (Fig. 2C), are bracketed by glaciogenic diamictites and apply directly to glacial climate conditions. Together with the existing age of 635.2 ± 0.6 Ma from the overlying Doushantuo cap carbonate (Condon et al., 2005), dated ~200 km to the north in the Three Gorges region, the ages from the Guzhang section suggest that the sampled Nantuo Formation was deposited in a short period of terminal Cryogenian time, potentially over less than 1 million years and representing prolonged deglaciation (Zhang et al., 2008a). Paleomagnetic sampling was carried out along the southeast limb of a late Jurassic-to-early Cretaceous anticline, with beds dipping gently to the southeast at 5–15° (Fig. 2A; HNBGMR, 1988).

Our other sampled section, here named Long'e section, is ~300 km south of the Guzhang section (Fig. 2B and D, near 25°49.2′N, 109°11.2′E). The Long'e section is close to Zhaoxing, a famous Dong People culture town in southeastern Guizhou Province (Fig. 1). The Nantuo Formation is more than 1000 m thick in this section (Fig. 2D). Lithologies sampled are typical basinal diamictite facies of the Nantuo Formation, predominantly green siltstone and mudstone matrix with pebbly dropstones. The base of the Nantuo Formation in this section is covered, but its upper contact with overlying Doushantuo cap carbonate is exposed. Sampling was carried out across the east limb of a syncline cored by Cambrian strata and overlain with angular unconformity by Carboniferous strata (Fig. 2B). Bedding dips steeply northwestward at 70–80°.

3. Paleomagnetic experiments and results

A total of 237 samples were collected from 12 sites using a gasoline-powered drill, including 97 siltstone–sandstone (redbed) samples from the Guzhang section and 140 fine- to medium-grained green-colored samples from the Long'e section. Samples were oriented using a magnetic compass and a sun compass when possible. Core samples were cut into ~0.7 cm thick specimens, excluding sizable dropstones if present.

Anisotropy of the magnetic susceptibility (AMS) for all specimens was first measured using a KLY-4S kappabridge in the paleomagnetic laboratory in China University of Geosciences, Beijing. Specimens were then subjected to stepwise alternating field (AF) and thermal demagnetization in the Yale University paleomagnetic laboratory. Remanent magnetizations were measured using a 2G superconducting magnetometer outfitted with automated sample changing capabilities (Kirschvink et al., 2008), and thermal demagnetization was carried out using a TD-48 thermal demagnetizer (ASC Scientific) in a N_2 atmosphere. AF demagnetization was carried out using a Molspin tumbling demagnetizer. Samples and instruments were kept in a μ-metal shielded room throughout the demagnetization process, with ambient magnetic fields typically 100–300 nT in the sample loading, transfer, and storage regions, and <10 nT in the magnetometer measurement and furnace heating/cooling zones. After natural remanent magnetization (NRM) measurements, low-field AF demagnetization (reaching peak alternating field of 15 mT stepwise by 2.5 mT) was applied. Then the samples were cooled and re-warmed in a shielded liquid N_2 basin through the Morin transition of hematite (258 K) and the Verwey transition of magnetite (120 K). These pre-treatments were considered to have removed viscous remanence carried by multi-domain particles of hematite or magnetite (Özdemir et al., 2002). After this procedure for all, the specimens were divided into different groups for further step-wise thermal

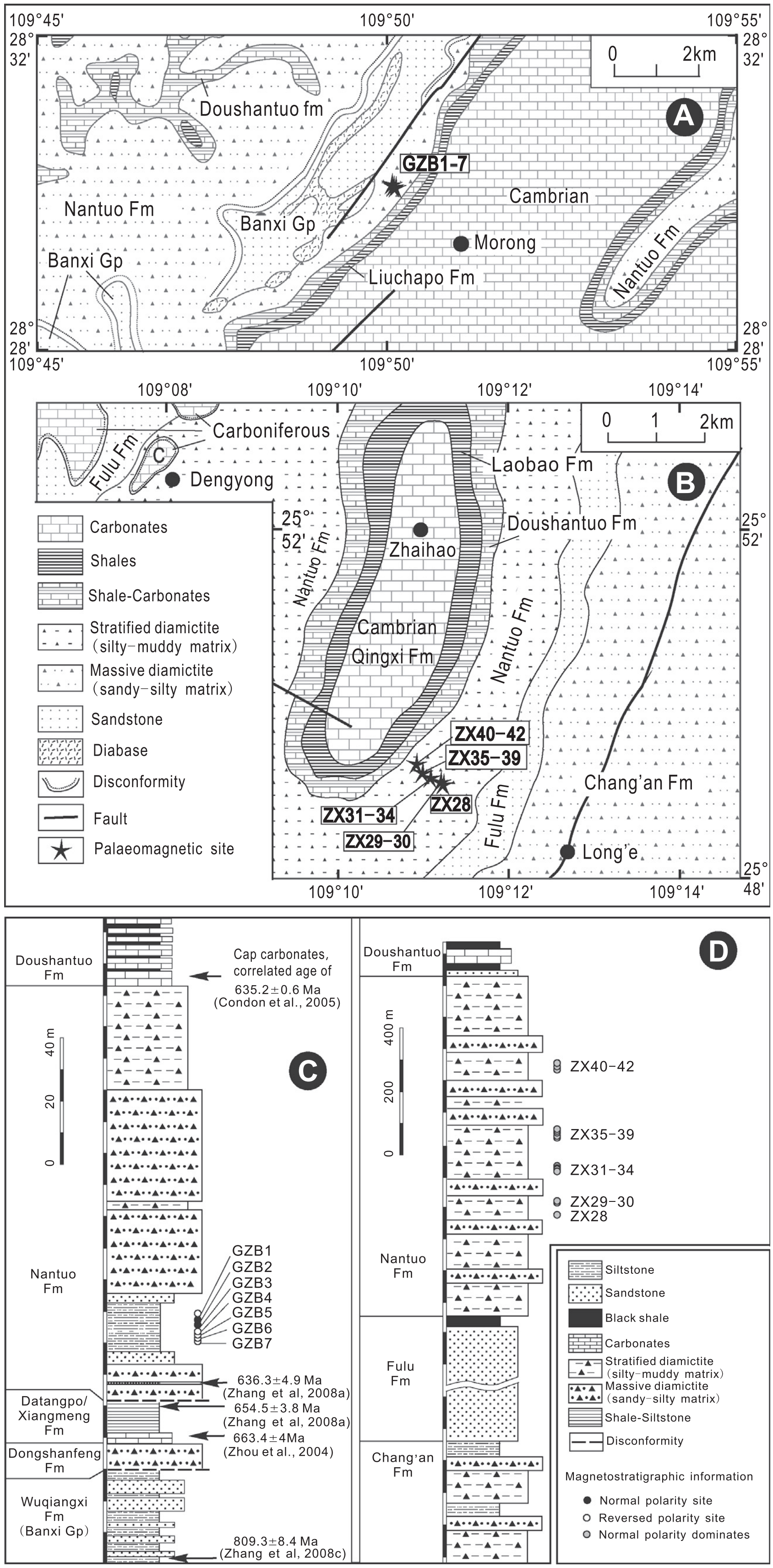

Fig. 2. Geological background of the paleomagnetic sampling sites. (A/B) geological maps for Guzhang/Long'e sections; (C/D) stratigraphic columns of Guzhang/Long'e areas. For paleomagnetic polarity zones, see Section 3 in text.

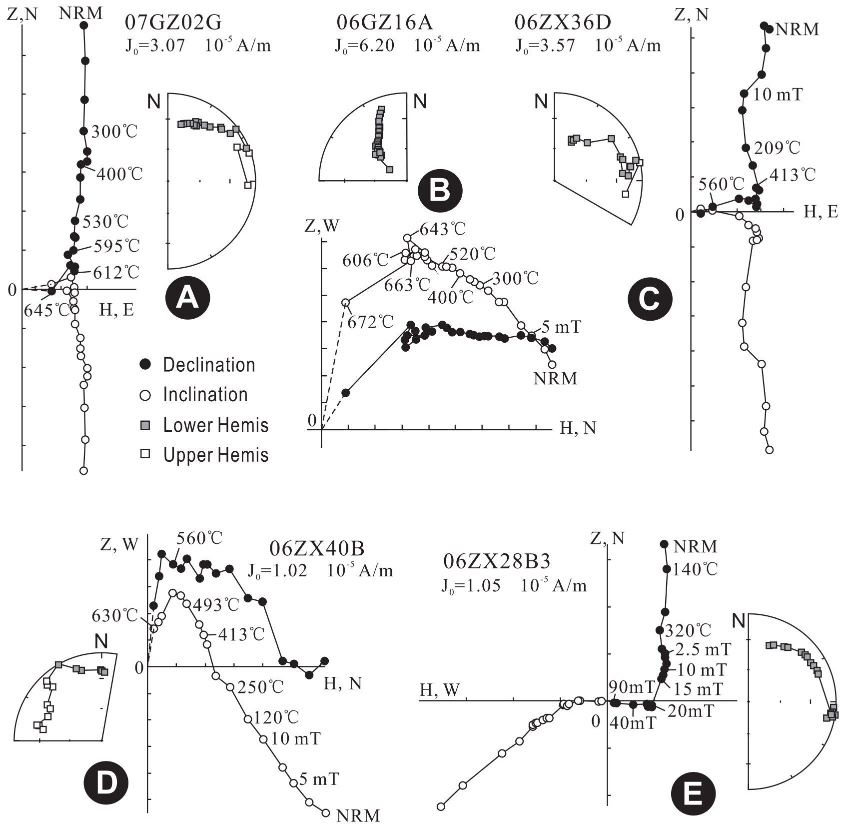

Fig. 3. Step-wise demagnetization plots of representative samples. (A) and (B) from Guzhang section and (C), (D) and (E) from Long'e section. NRM, natural remanent magnetization.

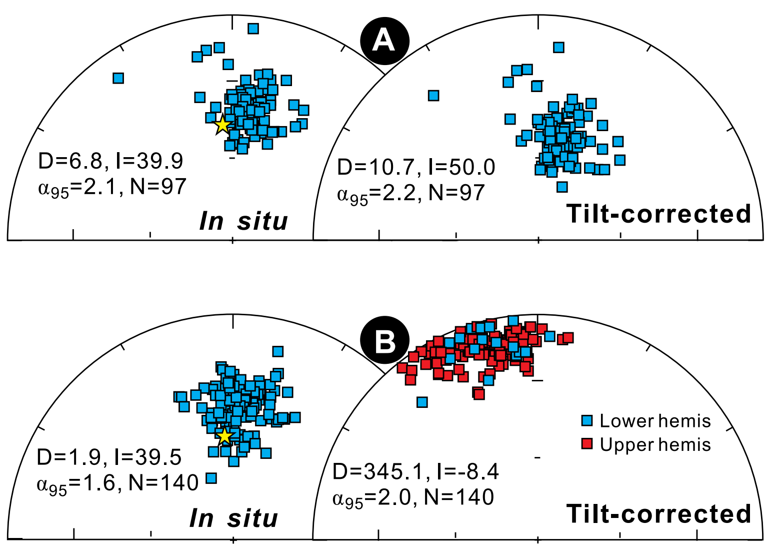

Fig. 4. Equal area projections of the soft component directions (A) from Guzhang section, and (B) from Long'e section. Stars showing the present geomagnetic field direction.

or AF demagnetization, or hybrid thermal-and-AF-combined methods. To identify the magnetic carriers, thermal demagnetization of a three orthogonal-axis isothermal remanent magnetization (IRM) was performed for representative samples following the Lowrie test (Lowrie, 1990).

3.1. Guzhang section

In the Guzhang section, the redbed natural remanent magnetization (NRM) intensities are 1–10 mA/m. Two components were identified using principal component analysis (Kirschvink, 1980). A magnetically soft component was removed mostly below 500 °C, concentrated around the present field direction of this region and hence regarded as a recent, viscous remanent magnetization (VRM) (Fig. 4A). A magnetically hard component with an unblocking temperature up to 672 °C was defined usually using a combined analysis of remagnetization great circles, yielding arc constraints with direct observations by stable endpoints, and high-temperature vectors decaying to the origin (McFadden and McElhinny, 1988). This component is dual-polarity (Fig. 5A), with

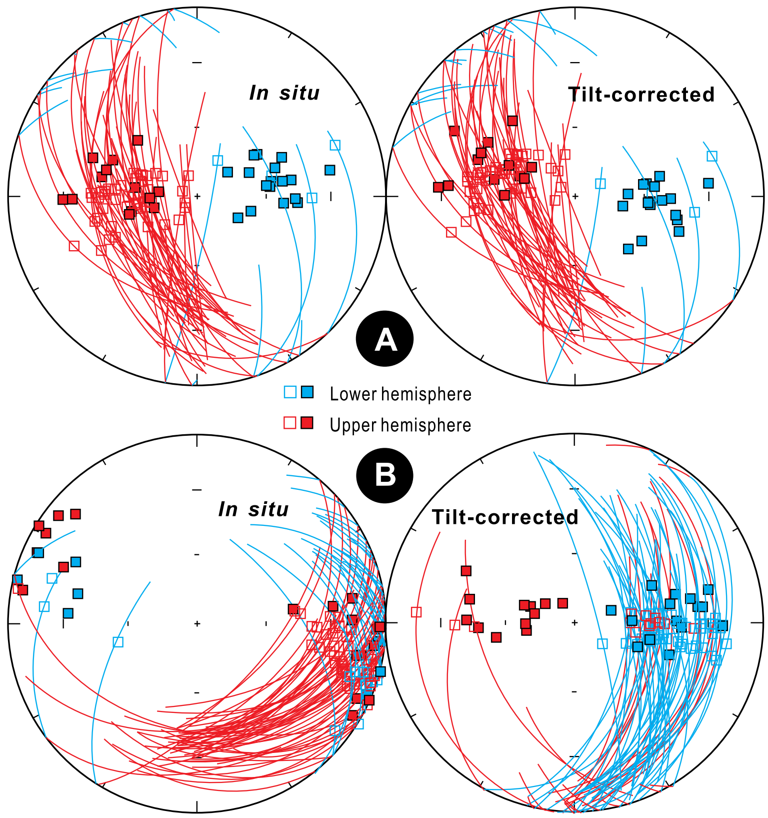

Fig. 5. Equal area projections of the hard component directions. Solid square is the direction defined by vector, open square on the arc is the direction defined by using a combined analysis of the great circle and direct observation. (A) Guzhang section, (B) Long'e section.

magnetization directed eastward and moderately down termed here as polarity 1 and magnetization directed westward and moderately up termed polarity 2.

One hundred percent of demagnetized specimens yielded usable constraints, with 30 characteristic remanent magnetizations (ChRM) fit by lines anchored to the origin and 48 fit using arc constraints. While vector-fit components are subequally divided between polarity 1 and 2, arc constraints are dominantly polarity 2, as expected, since the VRM overprint has downward inclination, closer to the polarity 1 direction. We note that the VRM is far removed from the polarity 1 direction defined both solely by vectors and dually by vectors and arc constraints (the overprint and the ChRM are separated by ~46°), whether in situ or in tilt-corrected coordinates. This affords confidence that arc constraints toward the ends of long remagnetization circles are not unduly biased toward the antipode of their overprint (i.e., as in Haggart et al., 2009). The unblocking-temperature range near to, but less than, the Neél temperature for hematite (~680 °C) suggests this ChRM is carried by detrital, low-Ti (originally magmatic) hematite or martite, and not by a fine-grained hematite pigment.

In the upper part of this sampled redbed interval, there are ~3.7-m-thick strata in which ChRMs are dominantly polarity 1, bounded by ~1.54-m-thick superjacent strata and ~6-m-thick subjacent strata dominated by polarity 2 (Fig. 2C). We regard this strata-bound remanence pattern as the record of two geomagnetic field reversals during deposition, only slightly modified by post-depositional, early diagenetic remanence processes. The directions pass a reversal test (Table 1) of "B" Class (McFadden and McElhinny, 1990).

AMS of these samples in the stratigraphic coordinates show that the minimum susceptibility (K_3) axes are perpendicular to the bedding plane, while the medium (K_2) and maximum (K_1) susceptibility axes lie in the bedding plane (Fig. 6A). Because there is no penetrative cleavage or deformation observed in the rock, this oblateness is likely of sedimentary magnetic fabric (Tarling and Hrouda, 1993). The K_2 and K_1 axes are segregated and the K_1 axes are roughly parallel to the regional fold axis, indicating these samples have a weak tectonic fabric (Parés et al., 1999). But there is no correlation between remanence components and the AMS principle axes. Stepwise thermal demagnetization of three orthogonal IRM components (Lowrie, 1990) for the redbed samples shows that each component, hard (2.5 T), medium (0.5 T) and soft (0.12 T), has a similar unblocking temperature around 675 °C (Fig. 7A). This strongly suggests that the major remanence carrier is hematite.

3.2. Long'e section

In the green-colored Long'e section, NRM intensities are mostly on the order of 1 mA/m. Demagnetization behavior is complex, indicating the samples contain multiple magnetic carriers. The samples can be roughly divided into two types. One type contains mainly magnetite with unblocking temperature close to 575 °C, determined by stepwise thermal demagnetization of NRM (Fig. 3C) and confirmed by thermal demagnetization of three-axis IRM (Fig. 7B). The other type contains non-negligible hematite, indicated by unblocking temperatures up to 675 °C during flowing-N_2 thermal demagnetization (Fig. 3D) and three-axis IRM thermal demagnetization (Fig. 7C). Sharp decay of the remanent magnetization and convergence of the hard-field and medium-field IRM demagnetization curves around 575 °C suggests that these samples also contain some magnetite grains. There is no significant stratigraphic pattern between these two types of samples. This variation in magnetic mineralogy may be due to wide and

Table 1
Paleomagnetic results for the Nantuo Formation in South China.

Site	Total, L C	N	$n^{E}n^{W}$	In geographic coordinates D (°)	I (°)	K	α_{95} (°)	Plat (°N)	Plon (°E)	dm/dp A_{95} (°)	In stratigraphic coordinates D (°)	I (°)	K	α_{95} (°)	Plat (°N)	Plon (°E)	dm/dp A_{95}(°)	RS/DIP (°)
Long'e section (25°49.2′N, 109°11.2′E)																		
ZX29–30	18, 6L12C	12	$8.5^{E}3.5^{W}$	100.7	−8.8	21.0	9.7	−11.6	198.5	9.8/4.9	84.8	47.8	21	9.7	16.4	174.4	12.6/8.2	219/67
ZX28	18, 8L10C	13	$9^{E}4^{W}$	113.4	−9.5	18.9	9.8	−23.1	193.0	9.9/5.0	102.1	54.1	18.9	9.8	5.3	163.0	13.7/9.6	219/67
ZX31–34	20, 3L17C	11.5	$11.5^{E}0^{W}$	103.0	−10.8	30.0	8.3	−14.1	198.4	8.4/4.2	89.3	47.7	30.0	8.3	12.7	173.0	10.8/7.0	219/67
ZX35–39	21, 6L15C	13.5	$10^{E}3.5^{W}$	279.7	27.2	20.6	9.2	−14.8	208.2	10.0/5.4	274.2	−47.7	20.6	9.2	8.7	171.3	11.9/7.8	206/78
ZX40–42	8, 4L4C	6	$3.5^{E}2.5^{W}$	104.9	7.9	37.1	11.1	−11.6	188.9	11.2/5.7	91.3	51.2	37.1	11.1	12.3	169.4	15.1/10.2	216/48
Average for Long'e section 5 sites				104.4	−9.7	36.1	10.4	−15.1	197.4	A_{95} = 8.0	92.1	49.8	263.5	3.9	11.1	170.2	A_{95} = 5.8	
Average using vector-component only, N = 27				105.6	−7.5	14.7	7.5	−15.7	195.8	7.5/3.8	90.7	53.3	19.3	6.5	13.4	167.8	9.0/6.3	
Guzhang section (28°30.1′N, 109°50.3′E)																		
GZB1	12, 3L9C	7.5	$0^{E}7.5^{W}$	264.2	−64.6	34.3	10.0	24.0	158.4	16.1/12.9	289.4	−56.3	31.8	10.4	3.0	158.9	15.0/10.8	67/16
GZB2	10, 6L4C	8	$6^{E}2^{W}$	74.0	60.6	25.8	11.1	29.9	165.8	16.9/12.9	98.7	55.5	26.4	11.0	10.0	164.1	15.7/11.2	68/16
GZB3	10, 8L2C	9	$9^{E}0^{W}$	76.3	50.9	28.0	9.9	25.3	176.0	13.4/9.0	88.7	51.5	28.8	9.8	15.7	171.4	13.3/9.0	86/10
GZB4	10, 2L8C	6	$2.5^{E}3.5^{W}$	76.8	61.3	25.1	13.6	28.0	164.3	21.0/16.1	93.1	61.0	25.1	13.6	16.5	160.5	20.9/16.0	83/9
GZB5	16, 5L11C	10.5	$1^{E}9.5^{W}$	278.2	−53.3	23.6	9.9	15.2	168.4	11.8/8.2	288.9	−50.1	23.9	9.8	5.6	165.9	11.3/7.7	83/9
GZB6	7, 2L5C	4.5	$0^{E}4.5^{W}$	272.5	−63.2	78.1	9.5	18.0	158.1	14.9/11.8	290.6	−58.8	73.4	9.8	3.7	156.1	14.5/10.8	78/11
GZB7	13, L4C9	8.5	$0.5^{E}8^{W}$	276.5	−55.2	28.8	10.1	11.4	165.2	14.4/10.2	288.1	−52.1	28.6	10.2	1.6	162.9	14.0/9.6	82/9
Average for Guzhang section 7 sites[a]				265.7	−58.8	114.2	5.0	20.8	165.1	A_{95} = 6.7	282.6	−55.3	155.2	4.3	8.0	162.8	A_{95} = 5.9	
Average using vector-component only, N = 30				87.3	56.3	26.5	5.2	18.6	167.3	7.5/5.4	102.6	52.8	28.6	5.0	5.9	164.8	6.9/4.8	
Average pole for Nantuo Formation on site-level[b]															9.3	165.9	A_{95} = 4.3	

Total, number of samples demagnetized, L, number of samples with vector component, C, number of samples with arc constraints only, N, number of samples for statistics (vector is weighted by 1, arc weighted by 0.5); n^{E}/n^{W}, numbers of directions towards east/west, D, declination, I, inclination; k, Fisher precision parameter of the mean; α_{95}/A_{95}, radius of circle of 95% confidence about the mean direction/pole. Plat/Plon, latitude/longitude of VGP; dp/dm, semi-axes of elliptical error around the pole at a probability of 95%, RS/DIP right hand strike/dip of the strata.

[a] Guzhang section passes a reversals test (McFadden and McElhinny, 1990), class B, with a Critical angle 7.1°, Different angle is 6.7°.

[b] Guzhang and Long'e results jointly pass a fold test by McFadden (1990), Definition 2.

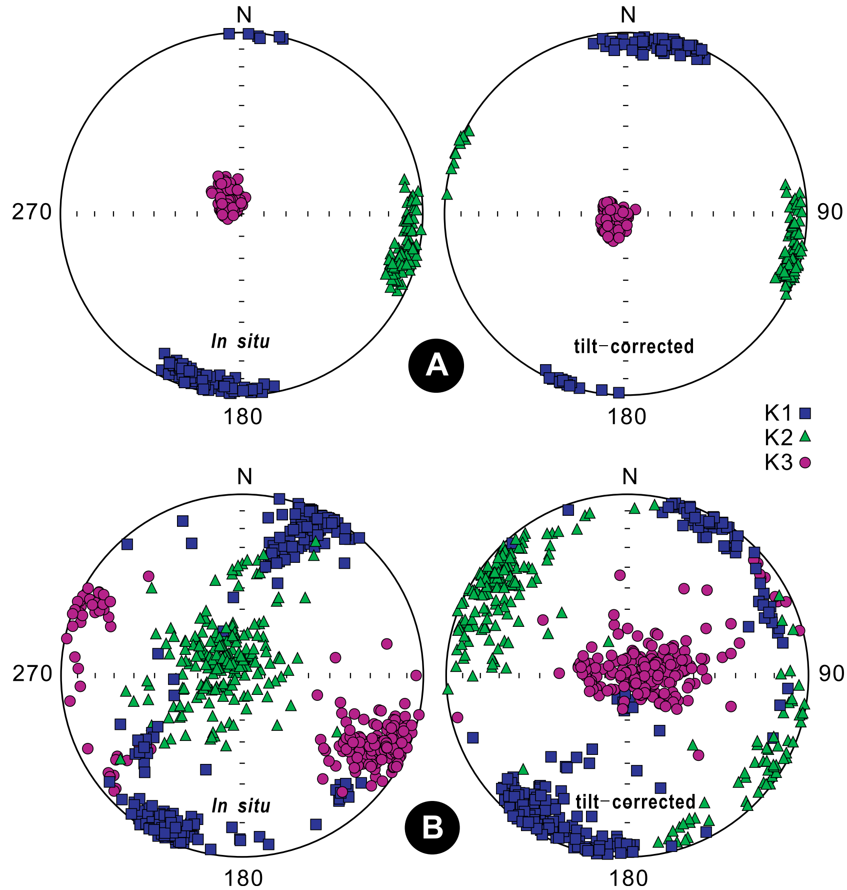

Fig. 6. Equal area projections of principle susceptibility axis directions for (A) Guzhang section, (B) Long'e section.

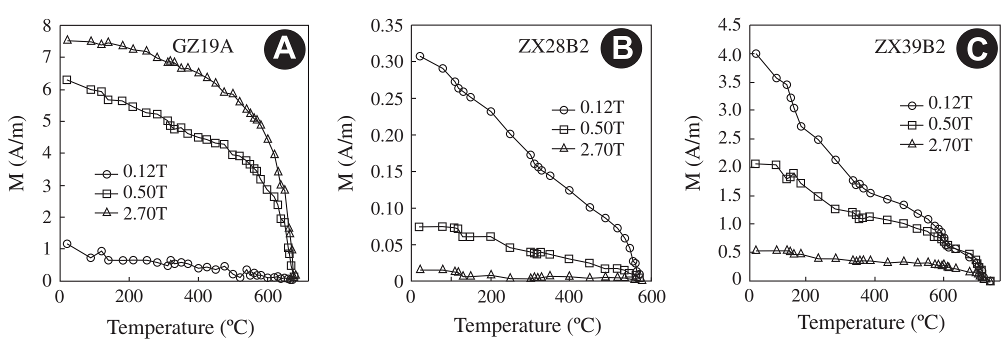

Fig. 7. Stepwise thermal demagnetization of the three orthogonal directions IRM (after Lowrie, 1990) for representative samples from (A) Guzhang section, (B) and (C) Long'e section.

complex provenance of sediments from the Nantuo ice sheets, preferentially expressed by uplands-averaging in the basin as opposed to proximal sources on the platform. It may also reflect centimeter-scale, variable diagenesis of originally oxidized components in the more anoxic basinal facies.

Vector line fitting combined with arc constraint analysis of remagnetization circles defined two components of NRM. Distribution of the soft component defined mostly below 500 °C resembles that of the Guzhang section in geographic coordinates (Fig. 4B). Both are close to the direction of the local present geomagnetic field and thus are regarded as a recent VRM. The Long'e hard component was defined during the last steps of demagnetization, mostly over 550 °C, both in the magnetite and hematite unblocking range, or between 20 and 90 mT (Fig. 3C–E). Magnetite at this temperature generally does not carry a viscous remagnetization. As at Guzhang, the Long'e hard component is dual-polarity.

One hundred percent of demagnetized specimens yielded usable constraints, with 27 ChRM's fit by lines anchored to the origin and 58 fit using arc constraints. While vector-fit components are, again, subequally divided between polarity 1 and 2 in similar tilt-corrected coordinate locations to the dual-polarity hard component at Guzhang (Fig. 5B), arc constraints from Long'e are dominantly polarity 1, whereas arc constraints from Guzhang are dominantly polarity 2. As at Guzhang, however, this pattern still is consistent with the hypothesis that arc constraints primarily reflect incompletely-removed VRM, because the steep attitude of the Long'e beddings brings the magnetization of polarity 2 in situ closer to the present geomagnetic field location than the magnetization of polarity 1 considered in situ. As at Guzhang, the Long'e VRM is far removed from the nearer in situ ChRM direction (separated by ~74°), affording confidence that arc constraints toward the ends of long remagnetization circles are truly approximating an ancient remanence more similar to the vector-defined ChRM than to the VRM antipode.

Dual-polarity directions occurred in most sampling sites. Considering both the multiple magnetic minerals in these samples and the relatively quick deposition rate presumed for these cryogenic sediments (Zhang et al., 2008a), we do not suggest that the strata in this section record geomagnetic field reversals in sequence. Instead we interpret that the hard component at Long'e may have been acquired by both depositional and diagenetic processes, albeit in a reversing geomagnetic field regime.

AMS measurements show that the K_3 axes are much more scattered than those observed from the Guzhang section, but they are still, to first order, orthogonal to the bedding plane, with a girdle distribution of the K_2 and K_1 axes (Fig. 6B). As there is no association between the principal susceptibility axes and the components of the NRM (Fig. 5B), we suggest that there is no significant tectonic deformation affecting the paleomagnetic directions from this section.

3.3. Combined results

We consider it significant that paleomagnetic results from these two sections are quite similar although lithologies and age of deformation are quite different. After removing the recent field remagnetization, the hard components from each section are separated by 72.2° in geographic (in situ) coordinates but converge to only 8.4° separation in tilt-corrected coordinates (with nominal α_{95}'s of ~4° each, though these somewhat underestimate the true uncertainty because of the non-circular distributions of our arc constraints) (Fig. 5A and B) (Table 1). These paleomagnetic results from Guzhang and Long'e sections jointly pass a McFadden (1990) fold test (Definition 2), indicating that the ChRM was acquired before Carboniferous time, defined by fold truncation at Long'e and by inference of similar magnetization at Guzhang, even though the strict fold-test age constraint in Guzhang is younger.

To the extent that our sampling of different lithologies (medium- to coarse-grained, detrital hematitic redbeds versus basinal, fine- to medium-grained, greenish-colored, diagenetic magnetite- and hematite-bearing mudstones) bears on the question of compaction-shallowing of paleomagnetic inclination, raised by Evans and Raub (2011) as a potential bias of low-paleolatitude "Snowball Earth" results, we fail to reject expectations. That is to say, our coarser-grained lithology is ~5.5° steeper-magnetized than our finer-grained lithology at a paleolatitude of maximum-expected effect (Kodama and Ward, 2001), despite a stronger sedimentary AMS fabric in the coarser-grained lithology. However, the combined magnetization uncertainties of both sites exceed 8°, so our difference is not statistically significant.

The site-mean paleomagnetic parameters are listed in Table 1. The site-level average paleomagnetic pole derived from the Long'e section is at (11.1°N, 170.2°E), A_{95} = 5.8°; the pole derived from the Guzhang section is at (8.0°N, 162.8°E), A_{95} = 5.9°. We combine these results (by averaging the virtual geomagnetic poles (VGPs) of each site in two sections) and obtain a site-mean pole at (9.3°N, 165.9°E), A_{95} = 4.3° for the Nantuo Formation we sampled.

This dual-site averaging approach is justified by comparison of predicted paleolatitudes on a site-specific basis versus predicted paleolatitudes from the all-VGP pole. The Long'e site-mean magnetization implies a paleolatitude of 30.7° ± 3.5°N for Long'e. The Guzhang site-mean magnetization implies a paleolatitude of 36.0° ± 4.4°N for Guzhang. Long'e and Guzhang are currently separated by 2.7° of arc, with basement-cored open folding suggesting only minor post-depositional shortening between the sites. Furthermore, the paleomagnetic declinations at both sites indicate that their paleo-positions would have been much closer in paleolatitude than paleo-longitude. Thus, unless minor tectonic rotations have affected the crustal cross-section between Long'e and Guzhang, a site-based approach yields an unsatisfying internal-consistency test. There is no evidence for significant vertical axis rotations in this region of the SCB.

By comparison, the dual-site, all-VGP pole predicts that Long'e lies ~270–300 km basinward of Guzhang at virtually the same latitude, ~34.0° ± 3.5°. This result is satisfyingly consistent with the current separation between our two sample sites and with the regional tectonic pattern in this part of the SCB.

For a technical comparison, we also calculate the paleomagnetic results using the only vector-fit data for the hard component, and list them in Table 1. The average directions and pole positions from such a calculation are almost identical to that of combined analysis of great circles and vectors. Only the combined analysis of circles and vectors can statistically pass a reversal test, although vectors from both sections obviously have dual polarities. We thus recommend the data using combined analysis for the final results in this paper.

3.4. Comparison with previous results

By this study, the Nantuo pole for the first time passes a strata-bound reversal test. It is comparable to the pole at (0.2°, 151.2°, dm = 7.5°, dp = 5.4°) previously obtained from the Nantuo Formation in Malong county, Yunnan Province (Zhang and Piper, 1997; Fig. 1), which passed a positive syn-sedimentary fold test. The site level VGPs of the Nantuo Formation from the three locations are in agreement with dual polarity, although some poles have considerable error ellipses (Fig. 8). We thus further suggest an average pole by combining all these site-level VGPs, at (7.5°N, 161.6°E), A_{95} = 5.9°, for the Nantuo Formation. The joint paleomagnetic results of the Nantuo Formation meet all the seven criteria of the paleomagnetic data reliability scale (Van der Voo, 1990), and this average pole therefore can be regarded as a key pole for the SCB at ~635 Ma.

The pole of the Nantuo Formation resembles that from the Liantuo Formation, yielding a medium paleolatitude for the SCB. However, it differs from the paleomagnetic results obtained from the Doushantuo Formation, which suggest an equatorial position for the SCB (e.g., Macouin et al., 2004). In fact, the eastward and shallow-directed component obtained from the Doushantuo Formation (Macouin et al., 2004) also exists widely in the Cambrian and Silurian strata in the SCB. This makes the primary origin of the Doushantuo pole questionable. In addition, only one polarity record was observed from the Doushantuo Formation throughout the entire Yangtze platform, in contrast with the paleomagnetic results obtained from early- to mid-Ediacaran successions in Australia (Sohl et al., 1999; Raub, 2008; Schmidt et al., 2009).

4. Paleogeographic implications

4.1. Connection between SCB and Cratonic Australia

During the past two decades, the relative positions of the SCB and Australia in the continental assemblages Gondwanaland and Rodinia have been actively discussed. In the "missing link model" of Rodinia reconstruction, Li et al. (1995, 2008b) suggested a position for the SCB in the center of Rodinia, connecting cratonic Australia and Laurentia. This model was inspired mainly by geological evidence, and was supported by a pair of paleomagnetic poles of ~820–810 Ma from the SCB (Xiaofeng dyke pole in Table 2) and

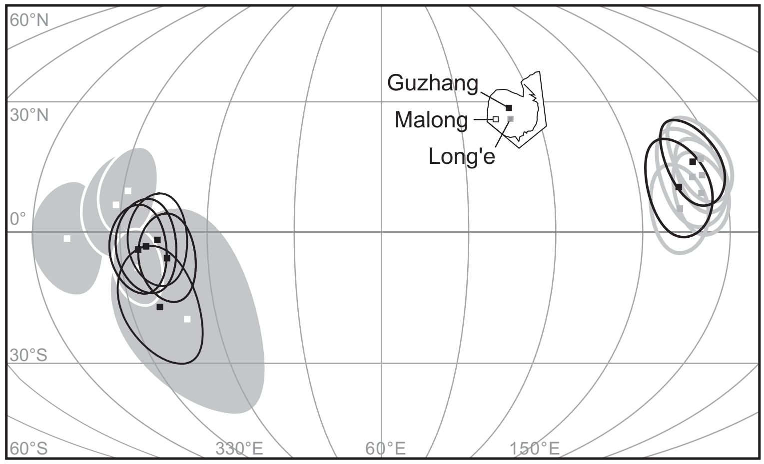

Fig. 8. Site-level Virtual Geomagnetic Poles (VGPs) obtained from the Nantuo Formation in the SCB. Ellipses of 95% confidence are drawn around each pole, black for the Guzhang section, gray for the Long'e section, white and gray shaded for the Malong section (Zhang and Piper, 1997). Sections located in the SCB are shown.

southern Australia (Wooltana Volcanics pole in Table 2). Subsequently, a pair of ~750 Ma paleomagnetic poles from the Liantuo Formation in South China (Evans et al., 2000) and from Mundine Well dykes in Western Australia (Wingate and Giddings, 2000) demanded that the "missing link model", if it ever had existed, must have broken apart by ~750 Ma. Those ~750 Ma poles may reconstruct the SCB either northeast or northwest of the cratonic Australia (Evans et al., 2000; Li et al., 2004; Li and Evans, 2011). By rotating three high quality poles, at ~750 Ma, middle Cambrian and Middle Silurian from the SCB to fit the coeval poles from Australia, together with paleobiogeographic evidence, Yang et al. (2004) proposed a long-lived connection (750–380 Ma) between

Table 2
Paleomagnetic poles selected for global reconstructions at ~750 Ma and ~635 Ma, and regional comparisons at ~550 Ma.

Age (Ma)	Pole	Rock unit	Plat (°N)	Plong (°E)	A_{95} (dm/dp) (°)	Notes and references
Australia						
~550	ARL	Arumbera sandstone, N Australia	53.9	168.1	8.8	Mitchell et al., 2010
~550	AEC	Arumbera sandstone	59.9	144.3	12.7	Mitchell et al., 2010
~550	IAR	L Arumbera Fm, U Pertatataka Fm	44.3	161.9	10.2	Grey and Corkeron, 1998; Kirschvink, 1978
600–635	Bra	Brachina Fm, S Australia	46	135.4	4.6/2.4	Schmidt et al., 2009
	Brb	Brachina Fm, S Australia	33	148	16	McWilliams and McElhinny, 1980
~635	NU	Nuccaleena Fm, S Australia	32.3	170.8	3.9/2.2	Schmidt et al., 2009
~635	EF	Elatina Fm, S Australia	43.7	179.3	4.2/2.1	Schmidt et al., 2009; Sohl et al., 1999
~635	YA	Yaltipena Fm, S Australia	44.2	172.7	11.4/5.9	Sohl et al., 1999
755 ± 4	MDS	Mundine Well dykes, W Australia	45	135	4	Wingate and Giddings, 2000
635–770	WTC	Walsh Tillite Cap carbonate, N Australia	22	102	14	Li, 2000
~820	WV	Wooltana Fm, S Australia	−62	142	17	McWilliams and McElhinny, 1980
Baltica						
616 ± 3	EG	Egersund Dolerites	−31.4	224.1	17/15	Walderhaug et al., 2007
Congo						
755	MB	Mbozi Complex	−46.0	145.0	9.0/5.0	Meert et al., 1995
India						
751–771	ML	Malani igneous suite	67.8	72.5	8.8	Gregory et al., 2009
Laurentia						
615 ± 2	LR	Long Range dykes	−19	175	18	Murthy et al., 1992; Kamo and Gower, 1994
742 ± 6	KF	Kwagunt Fm	18	166	7	Weil et al., 2004
North China Block (NCB)						
~650	DJ	Dongjia Fm	−60.8	97.4	6.7	Zhang et al., 2000
~700	HB	Mean pole for Huaibei Gp	−42.9	107.0	5.7	Zhang et al., 2006
800–780	NF	Nanfen Fm	−16.5	121.1	11.1	Lin, 1984
Siberia						
~760		~760 Ma dykes in S Siberia	1.3	22.1	6.9	Pisarevsky et al., 2010
South China Block (SCB)						
636 ± 5		Nantuo Fm	9.3	165.9	4.3	This study
		Nantuo Fm	0.2	151.2	7.5/5.4	Zhang and Piper, 1997
	NT	Average pole for ~635 Ma[a]	7.5	161.6	5.9	
748 ± 12		Liantuo Fm, CIT subset	3.4	163.6	2.7/2.1	Evans et al., 2000
		Liantuo Fm UWA subset	13.9	165.3	9.6/7.0	Evans et al., 2000
		Chengjiang Fm	2.2	153.4	13.1/9.4	Zhang and Piper, 1997
	LT	Average for ~750 Ma[a]	7.7	161.1	8.0	
802 ± 10	XF	Xiaofeng dykes	13.5	91	11.3/10.5	Li et al., 2004

Fm/Gp, Formation/Group; Plat/Plon, latitude/longitude of VGP; A_{95}, radius of circle of 95% confidence about the palaeopole. Other abbreviations are the same as in Table 1.
[a] Averaging all site VGPs from this formation and its equivalent. For more information about the averaged pole NT see Section **3.4**; for averaged pole LT see Section **4.1**.

the SCB and Australia, and placed the SCB against northwest Australia. Based on geochronological and geochemical data, Zhou et al. (2002) suggested that both the western and eastern margins of the YB were active arcs during the Neoproterozoic time and, therefore this block must have been an isolated continent surrounded by subduction zones. However, Jiang et al. (2003) argued that the modern eastern margin of YB in China may have been located close to northwestern India during the late Neoproterozoic time, because remarkably similar sedimentary facies assemblages exist in both the SCB and the Lesser Himalaya, from the rift-related siliciclastic–volcanic successions and glaciogenic rocks to the terminal Precambrian (Ediacaran) carbonate platform formations. Those authors also suggested that South China may have migrated toward northwestern Australia during the Cambrian, based on the stratigraphic and biogeographic analysis.

An SCB–Gondwanaland connection in the Paleozoic has been tested by fitting of their apparent polar wander paths (APWPs) (Zhang et al., 2001; Zhang, 2004; Macouin et al., 2004; Yang et al., 2004). Herein, we refine the Paleozoic APWP of the SCB by averaging high-quality middle Cambrian poles (Bai et al., 1998; Yang et al., 2004) and Middle-Late Silurian poles (Opdyke et al., 1987; Huang et al., 2000), respectively. Rotating the SCB to Africa 32° clockwise about a pole at (44.2°N, 352°E) may reasonably align the Cambrian to the Early-Middle Devonian APWPs of the SCB and Gondwanaland (Fig. 9). The best-fitted segments of the APWPs are those from early to middle Cambrian time (Fig. 9A, all plotted in Australia coordinates as north poles) and Silurian to Early Devonian time (Fig. 9B, all plotted in western Africa coordinates as south poles). Notwithstanding that the average Late Ordovician pole for Gondwanaland has considerable uncertainty (McElhinny et al., 2003), the rotated Ordovician pole from the SCB falls not far from the 490–450 Ma segment of Gondwana APWP. After 400 Ma, the two APWPs diverge markedly, indicating that the SCB commenced to rift from the Gondwanaland at this time (Fig. 9B). This reconstruction also is consistent with biogeographic and geological evidence (e.g. Burrett et al., 1990; Metcalfe, 1996), suggesting that the SCB attached along the northwest margin of Australia between Cambrian and Early Devonian time.

Our present compilation of the Precambrian paleomagnetic datasets permits to consider when such a SCB–Australia juxtaposition first formed. In Fig. 9A, we restore the Neoproterozoic poles from South and Western Australia to Northern Australia coordinates following the "Intraplate-rotation model" of Li and Evans (2011). Rotating the SCB to northern Australia using an Euler rotation (11.3°, 148.3°, 62.1°) as used in Fig. 9B, the Precambrian segments of the APWPs of these plates clearly demonstrate separation persisting until ~635 Ma at least. But in early Cambrian, when Gondwanaland had essentially amalgamated (Li and Powell, 2001; McElhinny et al., 2003; Trindade et al., 2006), paleomagnetic pole from the SCB falls close to the ~545 Ma pole of Gondwanaland (Fig. 9A). Because there is no high quality paleomagnetic pole available for the Ediacaran SCB thus far, a more tight constraint for the interval between ~635 Ma and 545 Ma is impossible.

Our analysis here differs from that of Yang et al. (2004), who proposed a long-lived SCB-Australia connection between ~750 and 380 Ma. This connection depends on their application of a ~20° CCW rotation to "correct" the pole from the Liantuo Formation, bringing it apparently closer to the coeval pole from Australian Mundine Well dykes.

After a careful review over the paleomagnetic datasets related to this issue, we suggest that such a correction of local rotation for the Liantuo pole is not conclusive. In the middle reaches of the Yangtze River, post-Triassic clockwise local rotations have been reported in several publications; but no evidence indicates that the Huangling dome-like batholith (HLB) region has been involved such a rotation. In an earlier study, Huang and Opdyke (1996) reported paleomagnetic results from the Badong region (31°N, 110.4°E), ~50 km west of the western margin of the HLB, indicating that a ~30° CW post-Triassic rotation occurred in this region with respect to other parts of the Yangtze block. One year later, the same research group (Huang and Opdyke, 1997) reported paleomagnetic results from the Jingdang region (31.4°N, 111.7°E), ~50 km east of the eastern margin of the HLB, and suggested that there is no significant local rotation observed in that region. Later, Shen et al. (1999) and Tan et al. (2007) identified a CW rotation up to ~30° in Xiangxi region (31°, 110.8°), which is ~10 km west of

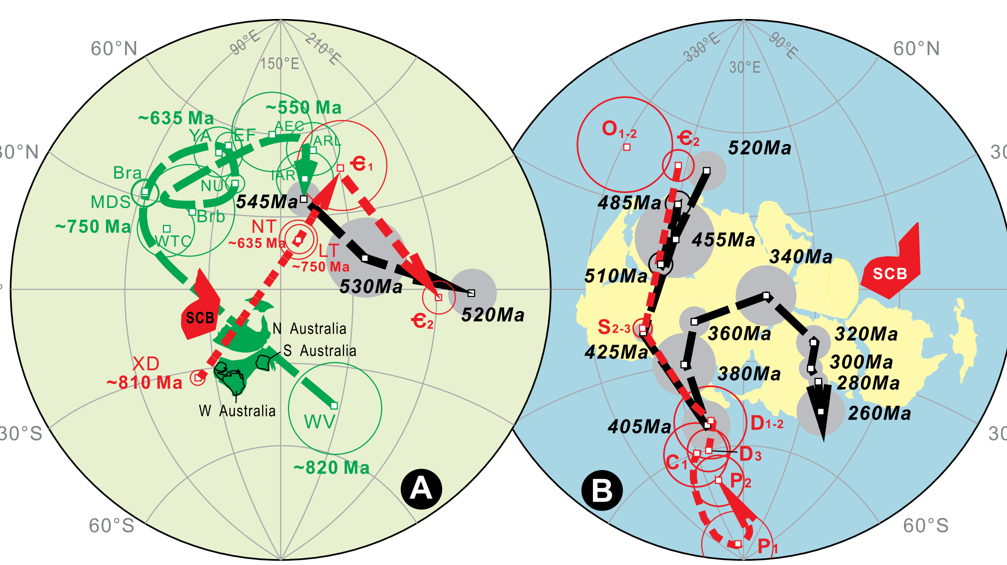

Fig. 9. APWPs fit between the selected paleomagnetic poles from the South China Block (SCB), Australian cratons, and Gondwana. (A) Australian cratons and their poles (all in green) are restored in present northern Australia coordinates following Li and Evans (2011), the SCB and its poles (all in red) rotated to Northern Australia using Euler rotation (11.3°, 148.3°, 62.1°), gray poles are from Gondwana following McElhinny et al. (2003), all are inferred as North poles and plotted in present northern Australian coordinates; for more information see Table 2 and text. (B) The SCB and its poles (in red) were rotated to Australia using Euler rotation (11.3°, 148.3°, 62.1°) as above, then all were plotted in present west Africa coordinates under reconstruction of Gondwana (Lawver and Scotese, 1987), matching the poles from Gondwana (in gray, following McElhinny et al., 2003). All poles are inferred as South poles. Middle Cambrian pole for the SCB is averaged on site level from Bai et al. (1998) and Yang et al. (2004), Middle-Late Silurian pole is averaged on site level from Opdyke et al. (1987) and Huang et al. (2000); for other poles and more comments see review in Zhang (2004). (For interpretation of the references to color in this figure legend, the reader is referred to the web version of this article.)

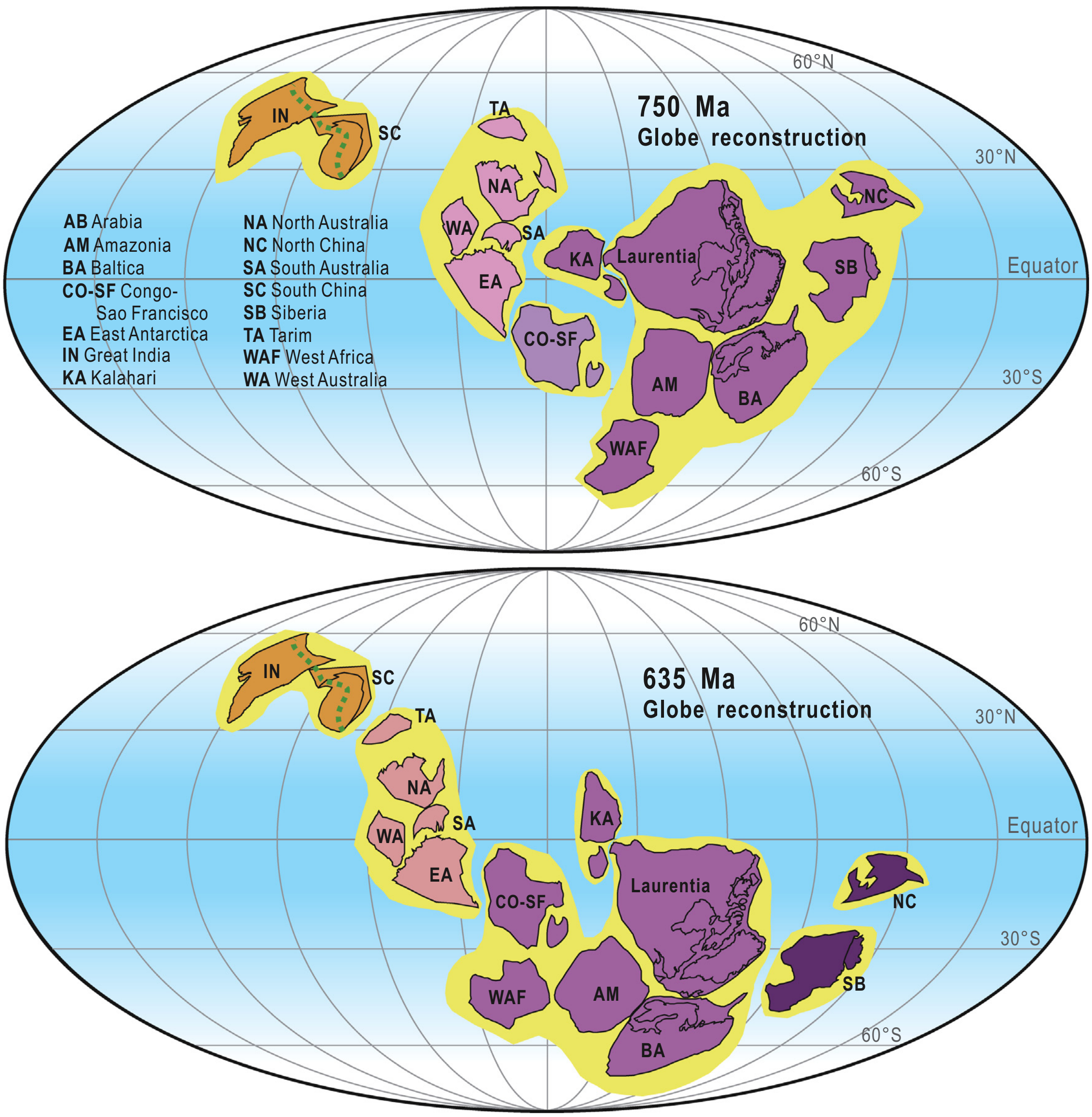

Fig. 10. Global reconstructions for ~750 Ma and ~635 Ma. For rotation parameters see Table 3; for further discussion see text. Green dashed line on the SCB and India shows the correlated rifted margin developed in late Neoproterozoic time. (For interpretation of the references to color in this figure legend, the reader is referred to the web version of this article.)

the HLB. The rotated and un-rotated regions in the middle reaches of the Yangtze River are apparently separated by the HLB.

The Xiaofeng dykes (802 ± 10 Ma) sub-vertically intruded the HLB (819 ± 7 Ma) (Li et al., 2004). The strata of the Liantuo Formation (748 ± 12 Ma) unconformably overlie the dykes and the batholith, and they are in turn disconformably overlain by the Nantuo glacial deposits, Ediacaran and Paleozoic strata. The following lines of evidence suggest that the HLB and its cover successions were not involved in the post-Triassic CW local rotation: (1) the early Cambrian paleomagnetic directions obtained from the Tianheban Formation in the HLB region are identical to that from the coeval Hetang Formation in Zhejiang Province, which is at the eastern end of the Yangtze platform, over 1000 km east of the HLB region (Lin et al., 1985). These results were reviewed by Zhang (2004) and are illustrated in this paper (Fig. 9A); (2) the Liantuo pole is indistinguishable from the coeval Chengjiang pole, and the Liantuo and Chengjiang formations are also over 1000 km apart (reviewed by Evans et al., 2000); (3) the Nantuo poles from central Hunan Province, East Guizhou Province and Chengjiang region of Yunnan Province are indistinguishable, indicating no rotation between these regions. The paired Liantuo–Nantuo poles and paired Chengjiang–Nantuo poles may further indicate that there was no rotation between HLB region, central Hunan Province, eastern Guizhou Province and Chengjiang region of Yunnan Province; and (4) the regional NS-striking faults (see Tan et al., 2007; Fig. 2) along the western margin of the HLB may reasonably mark the boundary of the CW-rotated region upstream of HLB, leaving them un-rotated. For these reasons, there is no compelling justification to apply any significant local-rotation-correction to the poles from Precambrian strata in the HLB region. Therefore, we further averaged all published VGPs from Liantuo and Chengjiang formations to get a mean pole (7.7°N, 161.1°E, A_{95} = 8.0°, N = 5) for the SCB around 750 Ma (Pole "LT" in Table 2).

Our paleomagnetic analysis favors a hypothesis in which the SCB was attached to the west side of cratonic Australia during the early Cambrian–Early Devonian interval, but had not yet

Table 3
Euler rotation parameters for 750 Ma and 635 Ma reconstructions.

	Euler rotation	Notes and references
750 Ma		
Amazonia to Laurentia (LA)	12, 313, −110.7	After Li et al. (2008b)
Baltica to LA	75.8, 264.2, −59.2	After Li et al. (2008b)
E Antarctica to Australia	−1.6, 39.2, 31.3	Lawver and Scotese (1987)
Great India to S China	22.2, 112.2, −117.1	Matching ~751–771 Ma Malani pole from India and pole LT from S China
Kalahari to LA	13.7, 326.5, −160.7	After Li et al. (2008b)
N China to LA	39, 87, 74	Based on Zhang et al. (2006)
Siberia to LA	67.5, 72.6, 153.3	Based on a 760 Ma pole newly reported by Pisarevsky et al. (2010)
Tarim to N Australia	13.5, 98.3, −153.4	After Li et al. (2008b); referred paleomagnetic result by Chen et al. (2004)
W Africa to LA	20.1, 334.1, −144.7	After Li et al. (2008b)
W and S Australia to N Australia	−20, 135, 40	Li and Evans (2011), Intraplate rotation within Australia 650–550 Ma
Congo and Sao Francisco	12.7, 90, 145.7	Based on Mbozi Complex pole (~755 Ma) (Meert et al., 1995)
LA	48.4, 201, −124.7	Based on Kwagunt (~742 Ma) pole (Weil et al., 2004)
N Australia	0, 1.6, 58.8	Based on Mundine Well dykes (~755 Ma) pole from W Australia (Wingate and Giddings, 2000)
S China	16.5, 86.1, 86.7	Based on pole LT, SCB (~750 Ma, Table 2)
635 Ma		
Amazonia to LA	12, 313, −110.7	After Li et al. (2008b)
Baltica to LA	75.8, 264.2, −59.2	After Li et al. (2008b), Matching paired poles of Long Range dyke VGP (~615 Ma) and Egersund dykes pole (~616 Ma)
Congo-Sao Francisco to LA	20.3, 333.1, −143.3	After Li et al. (2008b)
West Africa to LA	17.4, 328.3, −144.8	After Li et al. (2008b)
E Antarctica to Australia	−1.6, 39.2, 31.3	Lawver and Scotese (1987)
Great India to S China	22.2, 112.2, −117.1	Keep the 750 Ma connection, based on tectonostratigraphic correlation
Kalahari to LA	5.7, 136.1, 177.4	After Li et al. (2008b)
Tarim to N Australia	13.5, 98.3, −153.4	After Li et al. (2008b); keep the connection ~ 800 Ma
W and S Australia to N Australia	−20, 135, 40	After Li and Evans (2011), Intraplate rotation within Australia 650–550 Ma
Laurentia (LA)	0, 265, −109	Based on Long Range dyke VGP (~615 Ma)
N Australia	65.7, 75.5, 95.3	Based on the pole from Elatina Fm (Schmidt et al., 2009)
N China	12.7,67.4, 165.5	Based on the pole from Dongjia Fm (~650 Ma, Zhang et al., 2006)
S China	47.7, 145.1, 156.1	Based on the pole NT, SCB (~635 Ma, Table 2)
Siberia	27.6, 22.2, −161.4	Keep proximal position with LA and NCB

reached this position at ~635 Ma. The entire Ediacaran Period lacks reliable and well-dated paleomagnetic data to constrain the relationship between the SCB and Australia.

4.2. Chinese blocks in global context at ~750 Ma and ~635 Ma

The Late Neoproterozoic was a critical period in Earth history, for it witnessed the breakup of Rodinia, extreme climate changes and irreversible biospheric innovation. Global reconstruction is crucial to understanding the processes of these major geological events (e.g., Li et al., 2008b; Hoffman and Li, 2009). High-quality paleomagnetic poles from Liantuo and Nantuo formations, together with the high quality poles reported from other continents (Table 2), may improve the global reconstructions at ~750 Ma and ~635 Ma (Fig. 10; Euler Rotation parameters listed in Table 3).

The Malani pole (~771–751 Ma) and the ~750 Ma LT pole permit a tight juxtaposition of Greater India and the SCB (Fig. 10). This linkage is consistent with the tectonostratigraphic correlations in Jiang et al. (2003). Geological similarities between the Lesser Himalaya region and the SCB persisted from the preglacial Neoproterozoic, through both major glacial episodes, to the dominantly post-glacial Ediacaran Period; and from rift through drift phases of the sedimentary basins between ~750 and ~635 Ma. We therefore place Greater India and the SCB as a single plate in both ~750 Ma and ~635 Ma reconstructions (Fig. 10). Their positions at ~750 Ma and ~635 Ma were based on the LT and NT poles, respectively, placed between paleolatitudes of 30° and 60° in the north hemisphere for both times, with the Lesser Himalaya poleward of the SCB. The continuous margin between India and the SCB was essentially a meridional, east-facing trace, facing a northern paleo-ocean basin that probably was unbounded at those latitudes, especially during Marinoan time.

Three Neoproterozoic poles from the Tarim block have been reported recently (Chen et al., 2004; Huang et al., 2005; Zhan et al., 2007), but no consensus for its geographic position has been reached (e.g., Lu et al., 2008; Li et al., 2008b). We follow Li et al. (2008b) in attaching it to northern Australia mainly based upon geological correlations. During opening of the oceans between the hypothetically proximal landmasses of Australia and Laurentia, Tarim might reach a closest approach to the SCB at ~635 Ma (Fig. 10).

On the other side of our reconstruction, the position of the North China Block (NCB) at ~750 Ma was determined by matching its 800–700 Ma poles (pole NF and pole HB in Table 2) with the Kwagunt pole from Laurentia, notwithstanding poor age constraints for the poles from the NCB. Siberia is placed between the NCB and Laurentia, based on a new pole reported by Pisarevsky et al. (2010). By ~635 Ma, the NCB had rifted from Laurentia and Siberia, as evidenced by late Neoproterozoic successions developed along the present eastern and northern margins of the NCB (Zhang et al., 2006). Its paleogeographic position at ~635 Ma (Fig. 10) is based on a pole from the Dongjia Formation (Table 2), that immediately underlies the Luoquan tillite in the southern margin of the NCB.

The SCB is one of the cratons that best preserves the records of the assembly and breakup of Rodinia, extreme climate changes and Ediacaran-Cambrian "explosion" of the biosphere. In contrast, the NCB has a strikingly different geological history from that of the SCB, lacking records of all those geological events. Our reconstruction places the NCB and the SCB far apart from each other during late Neoproterozoic time, providing a paleogeographic explanation for the remarkable stratigraphic differences between the two blocks. Further study of the Tarim block and other Precambrian blocks in central and northeastern Asia would add constraints to this model.

5. Concluding remarks

In conclusion, we propose the following model for further testing: (1) New paleomagnetic results from the Nantuo Formation in South China identify reversals of the geomagnetic field during the relatively short period of terminal Cryogenian deglaciation. (2) The Nantuo glaciation occurred poleward of $\sim 30^{\circ}$ in northern hemisphere, on a meridional margin facing a wide paleo-ocean. (3) The SCB connected with the west side of Australia during the early Cambrian–Early Devonian, but it had not reached this position at $\sim$635 Ma. For the entire Ediacaran Period between $\sim$635 Ma and 542 Ma, there is no well-dated and reliable paleomagnetic data to constrain the geographic positions of the SCB.

Acknowledgements

This work was jointly supported by 973 Program (2011 CB808800), SinoProbe, China Geological Survey (1212010611808, 1212011120127), NSFC Projects 40921062, 40974035, 40032010B and 40830316. We are grateful for discussions with Profs. Ren Jishun, Gao Rui and Zheng-Xiang Li, and thank the constructive comments from Dr. Sergei Pisarevsky and Prof. Zhenyu Yang.

References

Bai, L., Zhu, R., Wu, H., Guo, B., Lu, J., 1998. New Cambrian paleomagnetic pole for Yangtze Block. Science in China, Series D 41 (Suppl.), 66–71.

Burrett, C., Long, J., Stait, B., 1990. Early-middle palaeozoic biogeography of Asian terranes derived from Gondwana. Geological Society, London, Memoirs 12 (1), 163–174.

Chen, Y., Xu, B., Zhan, S., Li, Y., 2004. First mid-Neoproterozoic paleomagnetic results from the Tarim Basin (NW China) and their geodynamic implications. Precambrian Research 133 (3–4), 271–281.

Condon, D., Zhu, M., Bowring, S., Wang, W., Yang, A., Jin, Y., 2005. U–Pb ages from the Neoproterozoic Doushantuo Formation, China. Science 308 (5718), 95–98.

Dobrzinski, N., Bahlburg, H., 2007. Sedimentology and environmental significance of the Cryogenian successions of the Yangtze platform, South China block. Palaeogeography, Palaeoclimatology, Palaeoecology 254 (1–2), 100–122.

Evans, D.A.D., Raub, T.D., 2011. Neoproterozoic glacial palaeolatitudes: a global update. In: Arnaud, E., Halverson, G.P., Shields-Zhou, G. (Eds.), The Geological Record of Neoproterozoic Glaciations, Geological Society, vol. 36. London, Memoirs, pp. 93–112.

Evans, D.A.D., Li, Z.X., Kirschvink, J.L., Wingate, M.T.D., 2000. A high-quality mid-Neoproterozoic paleomagnetic pole from South China, with implications for ice ages and the breakup configuration of Rodinia. Precambrian Research 100 (1–3), 313–334.

Gregory, L.C., Meert, J.G., Bingen, B., Pandit, M.K., Torsvik, T.H., 2009. Paleomagnetism and geochronology of the Malani Igneous Suite, Northwest India: implications for the configuration of Rodinia and the assembly of Gondwana. Precambrian Research 170 (1–2), 13–26.

Grey, K., Corkeron, M., 1998. Late Neoproterozoic stromatolites in glacigenic successions of the Kimberley region, Western Australia: evidence for a younger Marinoan glaciation. Precambrian Research 92 (1), 65–87.

Haggart, J.W., Ward, P.D., Raub, T.D., Carter, E.S., Kirschvink, J.L., 2009. Molluscan biostratigraphy and paleomagnetism of Campanian strata, Queen Charlotte Islands, British Columbia: implications for Pacific coast North America biochronology. Cretaceous Research 30 (4), 939–951.

HNBGMR (Hunan Bureau of Geology and Mineral Resources), 1988. Regional geology of Hunan Province. People's Republic of China Ministry of Geology and Mineral Resources Geological Memoirs, 8. Geological Publishing House, Beijing, 698 pp.

Hoffman, P.F., Li, Z.-X., 2009. A palaeogeographic context for Neoproterozoic glaciation. Palaeogeography, Palaeoclimatology, Palaeoecology 277 (3–4), 158–172.

Huang, K., Opdyke, N.D., 1996. Paleomagnetic of Middle Triassic redbeds from Hubei and northwestern Hunan Province, South China. Earth and Planetary Science Letters 143, 63–79.

Huang, K., Opdyke, N.D., 1997. Middle Triassic paleomagnetic results form central Hubei Province, China and their tectonic implications. Geophysical Research Letters 24, 1571–1574.

Huang, K., Opdyke, N.D., Zhu, R.X., 2000. Further paleomagnetic results from the Silurian of the Yangtze Block and their implications. Earth and Planetary Science Letters 175, 191–202.

Huang, B., Xu, B., Zhang, C., Li, Y., Zhu, R., 2005. Paleomagnetism of the Baiyisi volcanic rocks (ca. 740 Ma) of Tarim, Northwest China: a continental fragment of Neoproterozoic Western Australia? Precambrian Research 142 (3–4), 83–92.

Jiang, G., Wang, Z., Zhang, L., 1996. Sequence stratigraphy of upper Proterozoic glacigenic rocks in southeastern margin of Yangtze Platform. Journal of China University of Geosciences 7, 38–45.

Jiang, G., Sohl, L.E., Christie-Blick, N., 2003. Neoproterozoic stratigraphic comparison of the Lesser Himalaya (India) and Yangtze block (South China): paleogeographic implications. Geology 31 (10), 917–920.

Jiang, G., Kennedy, M.J., Christie-Blick, N., Wu, H., Zhang, S., 2006a. Stratigraphy, sedimentary structures, and textures of the late Neoproterozoic Doushantuo cap Carbonate in South China. Journal of Sedimentary Research 76 (7), 978–995.

Jiang, G., Shi, X., Zhang, S., 2006b. Methane seeps, methane hydrate destabilization, and the late Neoproterozoic postglacial cap carbonates. Chinese Science Bulletin 51 (10), 1152–1173.

Jiang, G., Shi, X., Zhang, S., Wang, Y., Xiao, S., 2011. Stratigraphy and paleogeography of the Ediacaran Doushantuo Formation (ca. 635–551 Ma) in South China. Gondwana Research 19 (4), 831–849.

Kamo, S.L., Gower, C.F., 1994. Note: U–Pb baddeleyite dating clarifies age of characteristic paleomagnetic remanence of Long Range dykes, southeastern Labrador. Atlantic Geology 30 (3), 259–262.

Kirschvink, J.L., 1978. The Precambrian–Cambrian boundary problem: paleomagnetic directions from the Amadeus Basin, Central Australia. Earth and Planetary Science Letters 40 (1), 91–100.

Kirschvink, J.L., 1980. The least-squares line and plane and the analysis of palaeomagnetic data. Geophysical Journal of the Royal Astronomical Society 62 (3), 699–718.

Kirschvink, J.L., Kopp, R.E., Raub, T.D., Baumgartner, C.T., Holt, J.W., 2008. Rapid, precise, and high-sensitivity acquisition of paleomagnetic and rock-magnetic data: development of a low-noise automatic sample changing system for superconducting rock magnetometers. Geochemistry Geophysics Geosystems 9 (5), Q05Y01.

Kodama, K.P., Ward, P.D., 2001. Compaction-corrected paleomagnetic paleolatitudes for Late Cretaceous rudists along the Cretaceous California margin: Evidence for less than 1500 km of post-Late Cretaceous offset for Baja British Columbia. Geological Society of America Bulletin 113 (9), 1171–1178.

Lawver, L.A., Scotese, C.R., 1987. A revised reconstruction of Gondwanaland. In: McKenzie, D. (Ed.), Gondwana Six: Structure, Tectonics and Geophysics, vol. 40. American Geophysical Union, Geophysical Monograph Series, pp. 17–24.

Li, Z.-X., 2000. New palaeomagnetic results from the 'cap dolomite' of the Neoproterozoic Walsh Tillite, northwestern Australia. Precambrian Research 100 (1–3), 359–370.

Li, Z.-X., Evans, D.A.D., 2011. Late Neoproterozoic 40° intraplate rotation within Australia allows for a tighter-fitting and longer-lasting Rodinia. Geology 39 (1), 39–42.

Li, Z.X., Powell, C.M., 2001. An outline of the palaeogeographic evolution of the Australasian region since the beginning of the Neoproterozoic. Earth-Science Reviews 53 (3–4), 237–277.

Li, Z.X., Zhang, L., Powell, C.M., 1995. South China in Rodinia: part of the missing link between Australia–East Antarctica and Laurentia? Geology 23 (5), 407–410.

Li, Z.X., Evans, D.A.D., Zhang, S., 2004. A 90° spin on Rodinia: possible causal links between the Neoproterozoic supercontinent, superplume, true polar wander and low-latitude glaciation. Earth and Planetary Science Letters 220 (3–4), 409–421.

Li, W.-X., Li, X.-H., Li, Z.-X., Lou, F.-S., 2008a. Obduction-type granites within the NE Jiangxi Ophiolite: implications for the final amalgamation between the Yangtze and Cathaysia Blocks. Gondwana Research 13 (3), 288–301.

Li, Z.X., Bogdanova, S.V., Collins, A.S., Davidson, A., De Waele, B., Ernst, R.E., Fitzsimons, I.C.W., Fuck, R.A., Gladkochub, D.P., Jacobs, J., Karlstrom, K.E., Lu, S., Natapov, L.M., Pease, V., Pisarevsky, S.A., Thrane, K., Vernikovsky, V., 2008b. Assembly, configuration, and break-up history of Rodinia: a synthesis. Precambrian Research 160 (1–2), 179–210.

Li, W.X., Li, X.H., Li, Z.X., 2010a. Ca. 850 Ma bimodal volcanic rocks in northeastern Jiangxi Province, South China: initial extension during the breakup of Rodinia? American Journal of Science 310 (9), 951–980.

Li, X.-H., Li, W.-X., Li, Q.-L., Wang, X.-C., Liu, Y., Yang, Y.-H., 2010b. Petrogenesis and tectonic significance of the ~850 Ma Gangbian alkaline complex in South China: evidence from in situ zircon U–Pb dating, Hf–O isotopes and whole-rock geochemistry. Lithos 114 (1-2), 1–15.

Lin, J.L., 1984. The Apparent Polar Wander Paths for the North and South China Blocks. Ph.D. Thesis, University of California Santa Barbara, 248pp.

Lin, J.L., Fuller, M., Zhang, W.Y., 1985. Paleogeography of the north and south China blocks during the Cambrian. Journal of Geodynamics 2, 91–114.

Lowrie, W., 1990. Identification of ferromagnetic minerals in a rock by coercivity and unblocking temperature properties. Geophysical Research Letters 17 (2), 159–162.

Lu, S., Li, H., Zhang, C., Niu, G., 2008. Geological and geochronological evidence for the Precambrian evolution of the Tarim Craton and surrounding continental fragments. Precambrian Research 160, 94–107.

Macouin, M., Besse, J., Ader, M., Gilder, S., Yang, Z., Sun, Z., Agrinier, P., 2004. Combined paleomagnetic and isotopic data from the Doushantuo carbonates, South China: implications for the ‘‘snowball Earth’’ hypothesis. Earth and Planetary Science Letters 224 (3–4), 387–398.

McElhinny, M.W., Powell, C.M., Pisarevsky, S.A., 2003. Paleozoic terranes of eastern Australia and the drift history of Gondwana. Tectonophysics 362 (1–4), 41–65.

McFadden, P.L., 1990. A new fold test for paleomagnetic studies. Geophysical Journal International 103, 163–169.

McFadden, P.L., McElhinny, M.W., 1988. The combined analysis of remagnetization circles and direct observations in palaeomagnetism. Earth and Planetary Science Letters 87 (1–2), 161–172.

McFadden, P.L., McElhinny, M.W., 1990. Classification of the reversal test in palaeomagnetism. Geophysical Journal International 103 (3), 725–729.

McWilliams, M.O., McElhinny, M.W., 1980. Late Precambrian Paleomagnetism of Australia: the Adelaide Geosyncline. The Journal of Geology 88 (1), 1–26.

Meert, J.G., Van der Voo, R., Ayub, S., 1995. Paleomagnetic investigation of the Neoproterozoic Gagwe lavas and Mbozi complex, Tanzania and the assembly of Gondwana. Precambrian Research 74 (4), 225–244.

Metcalfe, I., 1996. Gondwanaland dispersion, Asian accretion and evolution of eastern Tethys. Australian Journal of Earth Sciences 43 (6), 605–623.

Mitchell, R.N., Evans, D.A.D., Kilian, T.M., 2010. Rapid Early Cambrian rotation of Gondwana. Geology 38 (8), 755–758.

Murthy, G., Gower, C., Tubrett, M., Pätzold, R., 1992. Paleomagnetism of Eocambrian Long Range dykes and Double Mer Formation from Labrador, Canada. Canadian Journal of Earth Sciences 29 (6), 1224–1234.

Opdyke, N.D., Huang, K., Xu, G., Zhang, W.Y., Kent, D.V., 1987. Paleomagnetic results from the Silurian of the Yangtze paraplatform. Tectonophysics 139, 123–132.

Özdemir, Ö., Dunlop, D.J., Moskowitz, B.M., 2002. Changes in remanence, coercivity and domain state at low temperature in magnetite. Earth and Planetary Science Letters 194 (3–4), 343–358.

Parés, J.M., van der Pluijm, B.A., Dinarès-Turellb, J., 1999. Evolution of magnetic fabrics during incipient deformation of mudrocks (Pyrenees, northern Spain). Tectonophysics 307 (1–2), 1–14.

Pisarevsky, S.A., Gladkochub, D.P., Konstantinov, K., Mazukabzov, A., Stanevich, A., Tait, J.A., Donskaya, T.V., 2010. New Palaeomagnetic Data from the Kitoy River, South Siberia and applications to the Neoproterozoic palaeogeography. Geophysical Research Abstracts, vol. 12. EGU2010-3626, EGU General Assembly 2010.

Raub, T.D., 2008. Prolonged Deglaciation of Snowball Earth, Ph.D. Thesis, Yale University, New Haven.

Raub, T.D., Kirschvink, J.L., Evans, D.A.D., 2007. True polar wander: linking deep and shallow geodynamics to hydro- and bio-spheric hypotheses. In: Kono, M. (Ed.), Treatise on Geophysics, vol. 5. Elsevier, Amsterdam, pp. 565–589.

Schmidt, P.W., Williams, G.E., McWilliams, M.O., 2009. Palaeomagnetism and magnetic anisotropy of late Neoproterozoic strata, South Australia: implications for the palaeolatitude of late Cryogenian glaciation, cap carbonate and the Ediacaran System. Precambrian Research 174 (1–2), 35–52.

Shen, Z., Fang, D., Wang, P., Tan, X., Wang, Z., 1999. Paleomagnetism of early Triassic Daye Formation and its tectonic implications. Chinese Science Bulletin 44, 412–418.

Sohl, L.E., Christie-Blick, N., Kent, D.V., 1999. Paleomagnetic polarity reversals in Marinoan (ca. 600 Ma) glacial deposits of Australia: implications for the duration of low-latitude glaciation in Neoproterozoic time. Geological Society of America Bulletin 111 (8), 1120–1139.

Tan, X., Kodama, K.P., Gilder, S., Courtillot, V., Cogne, J.-P., 2007. Paleomagnetic evidence and tectonic origin of clockwise rotations in the Yangtze fold belt, South China block. Geophysical Journal International 168, 48–58.

Tarling, D.H., Hrouda, F., 1993. The Magnetic Anisotropy of Rocks. Chapman and Hall, London, 217 pp.

Trindade, R.I.F., D'Agrella-Filho, M.S., Epof, I., Brito Neves, B.B., 2006. Paleomagnetism of Early Cambrian Itabaiana mafic dikes (NE Brazil) and the final assembly of Gondwana. Earth and Planetary Science Letters 244 (1–2), 361–377.

Van der Voo, R., 1990. The reliability of paleomagnetic data. Tectonophysics 184 (1), 1–9.

Walderhaug, H.J., Torsvik, T.H., Halvorsen, E., 2007. The Egersund dykes (SW Norway): a robust Early Ediacaran (Vendian) palaeomagnetic pole from Baltica. Geophysical Journal International 168 (3), 935–948.

Wang, J., Li, Z.-X., 2003. History of Neoproterozoic rift basins in South China: implications for Rodinia break-up. Precambrian Research 122 (1–4), 141–158.

Wang, J., Li, X., Duan, T., Liu, D., Song, B., Li, Z., Gao, Y., 2003. Zircon SHRIMP U–Pb dating for the Cangshuipu volcanic rocks and its implications for the lower boundary age of the Nanhua strata in South China. Chinese Science Bulletin 48 (16), 1663–1669.

Weil, A.B., Geissman, J.W., Van der Voo, R., 2004. Paleomagnetism of the Neoproterozoic Chuar Group, Grand Canyon Supergroup, Arizona: implications for Laurentia's Neoproterozoic APWP and Rodinia break-up. Precambrian Research 129 (1–2), 71–92.

Wingate, M.T.D., Giddings, J.W., 2000. Age and palaeomagnetism of the Mundine Well dyke swarm, Western Australia: implications for an Australia–Laurentia connection at 755 Ma. Precambrian Research 100 (1–3), 335–357.

Yang, Z., Sun, Z., Yang, T., Pei, J., 2004. A long connection (750–380 Ma) between South China and Australia: paleomagnetic constraints. Earth and Planetary Science Letters 220 (3–4), 423–434.

Ye, M.-F., Li, X.-H., Li, W.-X., Liu, Y., Li, Z.-X., 2007. SHRIMP zircon U–Pb geochronological and whole-rock geochemical evidence for an early Neoproterozoic Sibaoan magmatic arc along the southeastern margin of the Yangtze Block. Gondwana Research 12 (1–2), 144–156.

Zhan, S., Chen, Y., Xu, B., Wang, B., Faure, M., 2007. Late Neoproterozoic paleomagnetic results from the Sugetbrak Formation of the Aksu area, Tarim basin (NW China) and their implications to paleogeographic reconstructions and the snowball Earth hypothesis. Precambrian Research 154 (3–4), 143–158.

Zhang, S., 2004. South China's Gondwana connection in the Paleozoic: paleomagnetic evidence. Progress in Natural Science 14 (1), 85–90.

Zhang, Q.R., Piper, J.D.A., 1997. Palaeomagnetic study of Neoproterozoic glacial rocks of the Yangzi Block: palaeolatitude and configuration of South China in the late Proterozoic Supercontinent. Precambrian Research 85 (3–4), 173–199.

Zhang, S., Li, Z.-X., Wu, H., Wang, H., 2000. New paleomagnetic results from the Neoproterozoic successions in southern North China Block and paleogeographic implications. Science in China Series D: Earth Sciences 43, 233–244.

Zhang, S., Zhu, H., Meng, X., 2001. New paleomagnetic results from the Devonian-Carboniferous successions in the Southern Yangtze Block and their paleogeographic implications. Acta Geologica Sinica 75 (3), 303–313.

Zhang, S., Jiang, G., Zhang, J., Song, B., Kennedy, M.J., Christie-Blick, N., 2005. U–Pb sensitive high-resolution ion microprobe ages from the Doushantuo Formation in South China: constraints on late Neoproterozoic glaciations. Geology 33 (6), 473–476.

Zhang, S., Li, Z.-X., Wu, H., 2006. New Precambrian palaeomagnetic constraints on the position of the North China Block in Rodinia. Precambrian Research 144 (3–4), 213–238.

Zhang, S., Jiang, G., Han, Y., 2008a. The age of the Nantuo Formation and Nantuo glaciation in South China. Terra Nova 20 (4), 289–294.

Zhang, Q.R., Li, X.H., Feng, L.J., Huang, J., Song, B., 2008b. A new age constraint on the onset of the Neoproterozoic glaciations in the Yangtze Platform, South China. Journal of Geology 116, 423–429.

Zhang, S., Jiang, G., Dong, J., Han, Y., Wu, H., 2008c. New SHRIMP U–Pb age from the Wuqiangxi Formation of Banxi Group: implications for rifting and stratigraphic erosion associated with the early Cryogenian (Sturtian) glaciation in South China. Science in China Series D: Earth Sciences 51 (11), 1537–1544.

Zhang, Q.R., Chu, X.L., Feng, L.J., 2011. Neoproterozoic glacial records in the Yangtze region, China (*in* The geological record of Neoproterozoic glaciations). Memoirs of the Geological Society of London 36, 357–366.

Zhang, S.-B., Wu, R.-X., and Zheng, Y.-F., in press. Neoproterozoic continental accretion in South China: geochemical evidence from the Fuchuan ophiolite in the Jiangnan orogen. Precambrian Research. http://dx.doi.org/10.1016/j.precamres.2012.07.010.

Zhao, J.-H., Zhou, M.-F., Yan, D.-P., Zheng, J.-P., Li, J.-W., 2011. Reappraisal of the ages of Neoproterozoic strata in South China: no connection with the Grenvillian orogeny. Geology 39 (4), 299–302.

Zhou, M.-F., Yan, D.-P., Kennedy, A.K., Li, Y., Ding, J., 2002. SHRIMP U–Pb zircon geochronological and geochemical evidence for Neoproterozoic arc-magmatism along the western margin of the Yangtze Block, South China. Earth and Planetary Science Letters 196 (1–2), 51–67.

Zhou, C., Tucker, R., Xiao, S., Peng, Z., Yuan, X., Chen, Z., 2004. New constraints on the ages of Neoproterozoic glaciations in South China. Geology 32 (5), 437–440.